Article ID: 1003- 6326(2000)01- 0014- 05

Skull formation and change during ISM process of Ti-15-3 alloy①

GUO Jing-jie(郭景杰), LIU Yuan(刘 源),
SU Yan-qing(苏彦庆), DING Hong-sheng(丁宏升), JIA Jun(贾 均)
School of Materials Science and Engineering, Harbin Institute of Technology, Harbin 150001, P. R. China

Abstract: The change of the skull shape and size has been predicated through computer simulation technique and compared with the experimental results. The microstructure of the skull and the elemental line distribution in the skull have been analyzed with optical microscope and EPMA etc. The results show that the skull height and thickness become small with increasing melting power; the skull consists of two zones, that is, fine equiaxial crystal zone and coarse columnar crystal zone; there exists some segregation in the bottom of the skull.

Key words: Ti-15-3 alloy; skull melting; microstructure segregation **Document code:** A

1 INTRODUCTION

Metastable β titanium alloys are now finding more extensive applications, especially owing to their good forming properties. Ti-15V-3Cr-3Al-3Sn (Ti-15-3), a typical metastable β titanium alloy, was developed to answer the need for a titanium alloy sheet metal in aerospace application. In addition, due to its more excellent casting character than that of traditional Ti-6Al-4V alloy, its castings have been used widely in aircraft structures with high strength substituting stainless steel[1~3].

Induction skull melting (ISM) process has been promoted as a method of producing clean titanium ingot or powder and it is an advanced process combining the advantages of induction melting technique and cold-wall melting technique for melting high reactivity alloys[4~6]. During the melting process, the strong electromagnetic stirring action in the molten metal guarantees the homogeneity of alloy composition. At the same time, as shown in Fig. 1, a layer of skull formed from resolidified metal between the molten metal and the crucible prevents the molten metal from the contamination caused by the crucible material. But just due to the existence of the skull, once the alloying elements appear in enrichment or poverty in the skull, the composition of the obtained ingot would undoubtedly deviate from the ideal value. So studying the formation mechanism of the skull as well as macro-segregation of elements in it is very essential for getting ideal material composition and good mechanical properties. Thus it is the purpose of the present paper to understand the skull forming process and the effect of skull on the melt composition, which would be a guide for eliminating the segregation of the elements in the skull.

2 EXPERIMENTAL

The melting of Ti-15-3 alloy was performed in an induction skull melting furnace with a copper crucible of 1.3 L. Two melting practices were conducted and the applied power is shown in Table 1. The vacuum degree is about 1.2 Pa. The original states of these raw materials are sponge titanium, pure Cr (powder), pure Sn (block) and $V_{0.85}Al_{0.15}$ master-alloy (particle). First Ti and $V_{0.85}Al_{0.15}$ were mixed together and put into the crucible as the lowest layer of the charge. Then Cr powder was put on the top. For Sn element, in order to avoid its enrichment in the skull in virtue of its low melting-point, it was not charged until the raw materials in the crucible had been melted partly.

After the melting process, the microstructure of the skull was observed with optical microscope and the composition of the skull as well as the ingot was analyzed by chemical analysis method. In addition, the elemental distribution in the skull was measured with an electron probe micro analyzer (EPMA).

3 RESULTS AND DISCUSSION

3.1 Change of skull shape and size during melting process

During the melting process, because the skull in the crucible is invisible, the shape and size of the skull can not be observed. In order to get a well understanding of the changing process, the temperature field in the charge had been simulated (the applied numerical model had been reported in Refs. [7] and [8]). As a result of the simulation, the skull shape and size at any moment can be got. In the simulating calculation, except that the simulated charge is Ti-15-

① **Foundation item:** Project supported by the Science Foundation of China for Outstanding Young Teachers
Received date: Dec. 21, 1998; **accepted date:** Mar. 30, 1999

3 alloy ingot, the other parameters including the melting power(Fig. 2), the melting time (600 s) as well as the charge mass are the same as those used in the melting practices mentioned above.

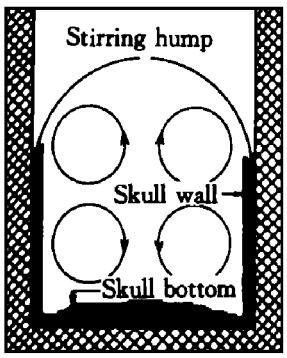

Fig. 1 Diagram of induction skull melting process

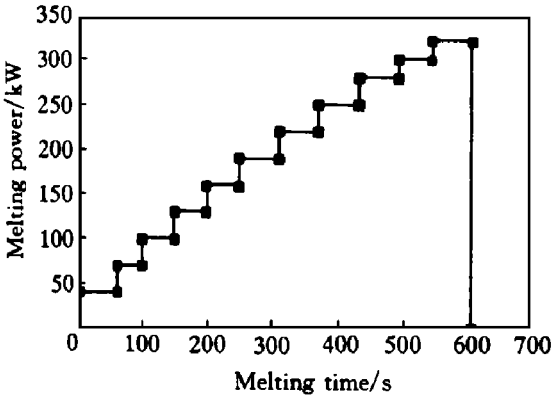

Fig. 2 Change of melting power during melting practice of Ti-15-3 alloy

The simulated results —the changing relationship between the shape, size of the skull and the melting time are shown illustratively in Fig. 3(only half of the skull is drawn because of its axial symmetry). As can be seen from Fig. 3, during the melting process, the thickness of the skull wall decreases slowly with increasing input power. In fact, its thickness drops from 1.7 mm at 200 kW(300 s) to 0.9 mm at 320 kW (600 s); also its height falls continuously for the fact that the increasing power makes the stirring hump higher and higher. Compared with the skull wall, the skull bottom shows a remarkable change in its thickness and shape because, in the cylindrical charge, the produced induction heat increases with the rise of the radius; in addition, the cooling water has the same intensity of cooling to the skull bottom. So in the prephase of the melting process, the skull bottom appears as wedge shape as that in Fig. 3(a). But in the anaphase of the melting process, due to the high temperature and the intensive stirring action in the molten pool, the heat transfers at a high speed; as a result, the skull bottom becomes more and more flat and in the end, the average thickness of the skull bottom is about 1.4 mm.

The true skull obtained from the melting practice is shown in Fig. 4 and Table 1 lists the measured thicknesses of various parts of it. Compared with the simulated results in Fig. 3, the experimental results in Table 1 are higher. The deviation can be explained from this point —when the melt next to the skull flows along the skull surface during the pouring process, it solidifies and sticks to the original skull due to its lower flowing ability caused by the disappearance of inner heat source and its lower temperature in itself.

3.2 Microstructure of skull

The microstructure of the skull is shown in Fig. 5. It can be observed clearly from Figs. 5(a) and (b) that, on the whole, the microstructure of the skull includes two parts, namely very fine equiaxial crystal zone and coarse columnar crystal zone. The fine equiaxial crystal zone is located in the outer side of the skull and identified as "*A*" where the equiaxial crystal is not visible because the crystal is very fine and at the same time, the magnification times of the optical microscope is not large enough. The coarse equiaxial crystal zone is located in the inner side of the skull and identified as "*B*" zone. In addition, in the skull bottom, some unmelted titanium particles and holes can be observed in the lower position, but to the skull wall, there does not exist this kind of phenomenon. The cause lies in the different formation process of the skull wall and skull bottom which will be discussed in the following section 3.4.

During the melting process, when the liquid melt touches the crucible, due to the shock cooling action of the crucible to the melt, a layer of solid skull made of very fine chill crystals is formed, which is the fine equiaxial zone shown in Fig. 1. Just next to the solid skull is the solid+liquid phase where the crystals grow parallelly to the reverse direction of the heat flux and in the end forms the columnar crystal zone. Due to the strong stirring action in the inner melt, the liquid+solid phase next to the solid+liquid phase fades.

3.3 Macro-segregation of alloying elements in skull

Macro-segregation of alloying elements in skull is a determining factor causing the composition of the melt to deviate from the nominal composition. Therefore reducing the macro-segregation of alloying elements in the skull is an important task that must be accomplished during the ISM process. From the data in Table 2 —the average contents of alloying elements in the skull(the sampling positions shown in Fig. 4) and ingot(because in the ingot the composition is homogeneous[9], so the sampling position can be selected arbitrarily), it can be found that there exists little macro-segregation in the skull wall because that the contents of these four elements —V, Al, Cr and Sn, are equal to those in the ingot; but in the skull bottom, there exists almost segregation of all alloying el-

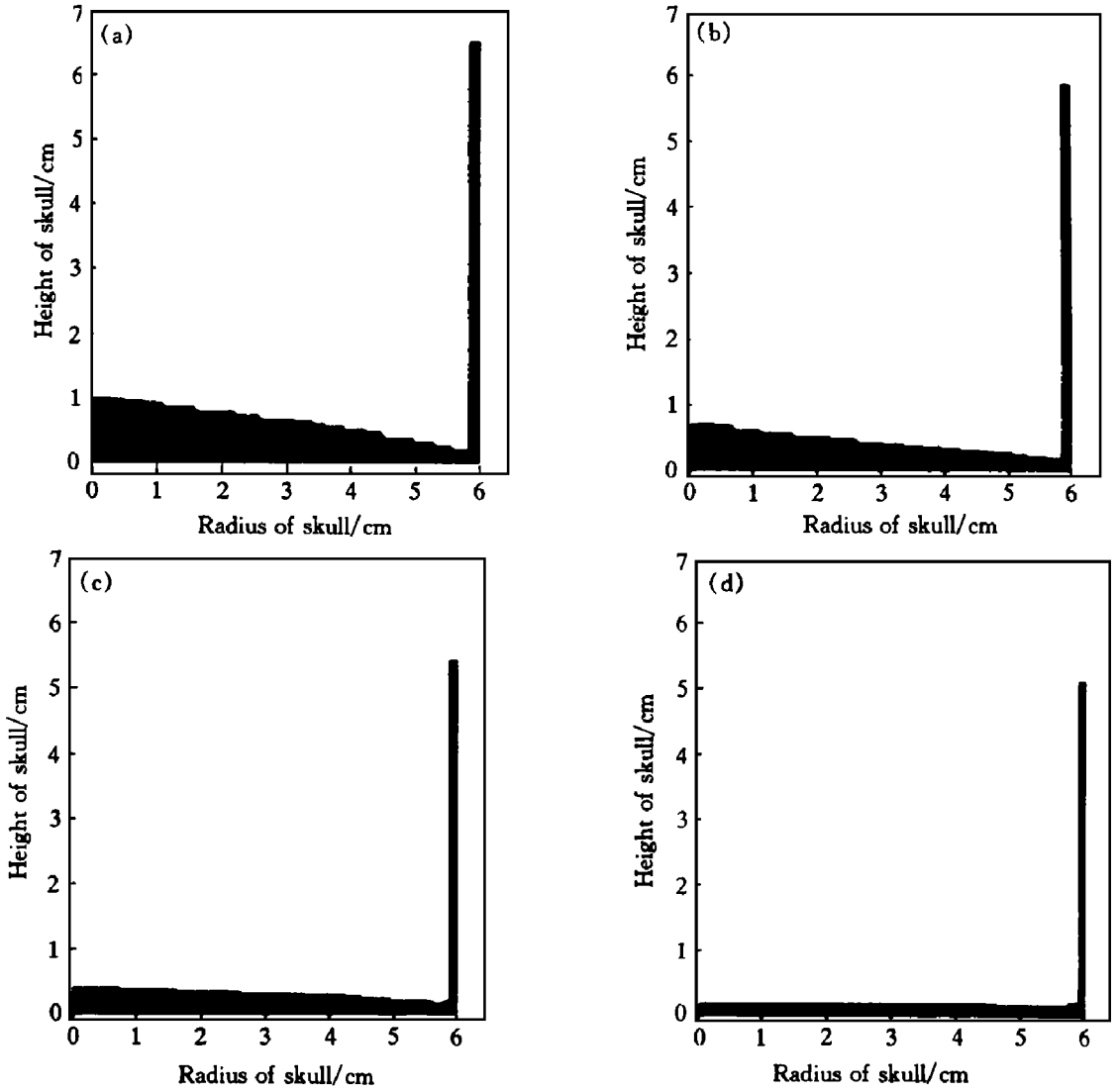

Fig. 3 Change of skull size and shape during ISM process of Ti-15-3 alloy
(Here the skull is thought as the part where the solid ratio is not less than 0.5.)
(a) —Melting time= 300 s; (b) —Melting time= 400 s; (c) —Melting time= 500 s; (d) —Melting time= 600 s

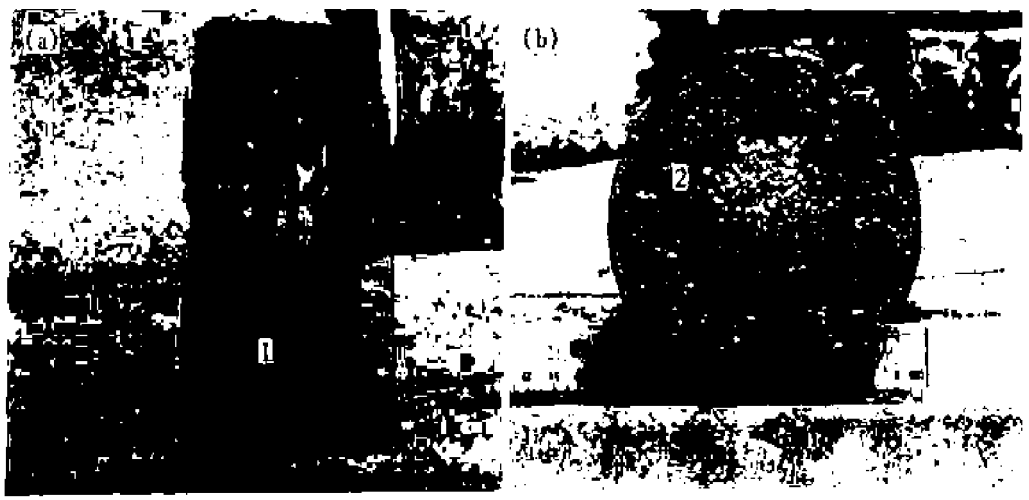

Fig. 4 Photographs of Ti-15-3 skull formed during ISM process
(a) —Skull wall; (b) —Skull bottom

ements and concretely, the most serious segregation happens to Cr element and the next serious segregation happens to Sn element, to the other two elements of Al and V, their segregation is slight.

In addition, according to Figs. 6(a), (b) and (c) —the line distribution of alloying elements in the skull bottom, in the skull wall and in the ingot, respectively, it can be found that there are concentra-

Table 1 Thickness of various parts of skull obtained from real melting practices

Number of melting practices	Charge mass /kg	Melting power /kW	Vacuum degree /Pa	Thickness of skull wall /mm	Thickness of skull bottom/mm	
					$r=0$	$r=5$ cm
Number 1	5.5	Fig. 3	1.2	1.7	2.2	2.0
Number 2	5.2		1.3	1.8	2.3	2.0

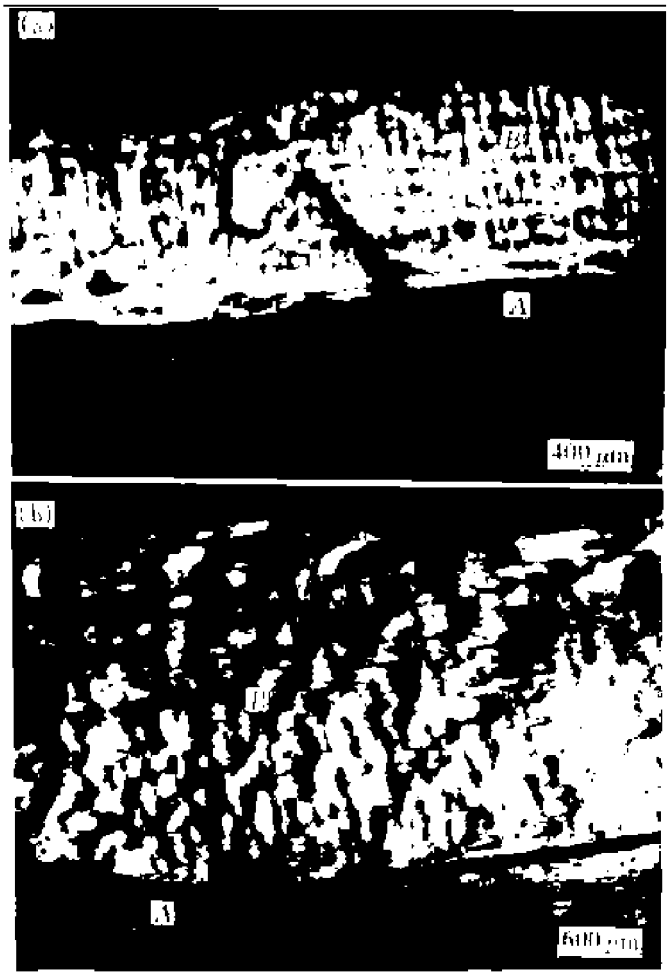

Fig. 5 Cross-sectional microstructures of skull
(a) —Skull wall; (b) —Skull bottom
A —fine equiaxial crystal zone;
B —coarse columnar crystal zone

Table 2 Compositions of Ti-15-3 alloy skull and ingot (%)

Composition	Ingot	Skull	
		Bottom	Wall
V	14.54	14.45	14.50
Cr	2.74	2.89	2.75
Al	2.85	2.84	2.86
Sn	2.84	2.79	2.83

The sampling positions are shown in Fig. 4, where 1 —skull wall, 2 —skull bottom

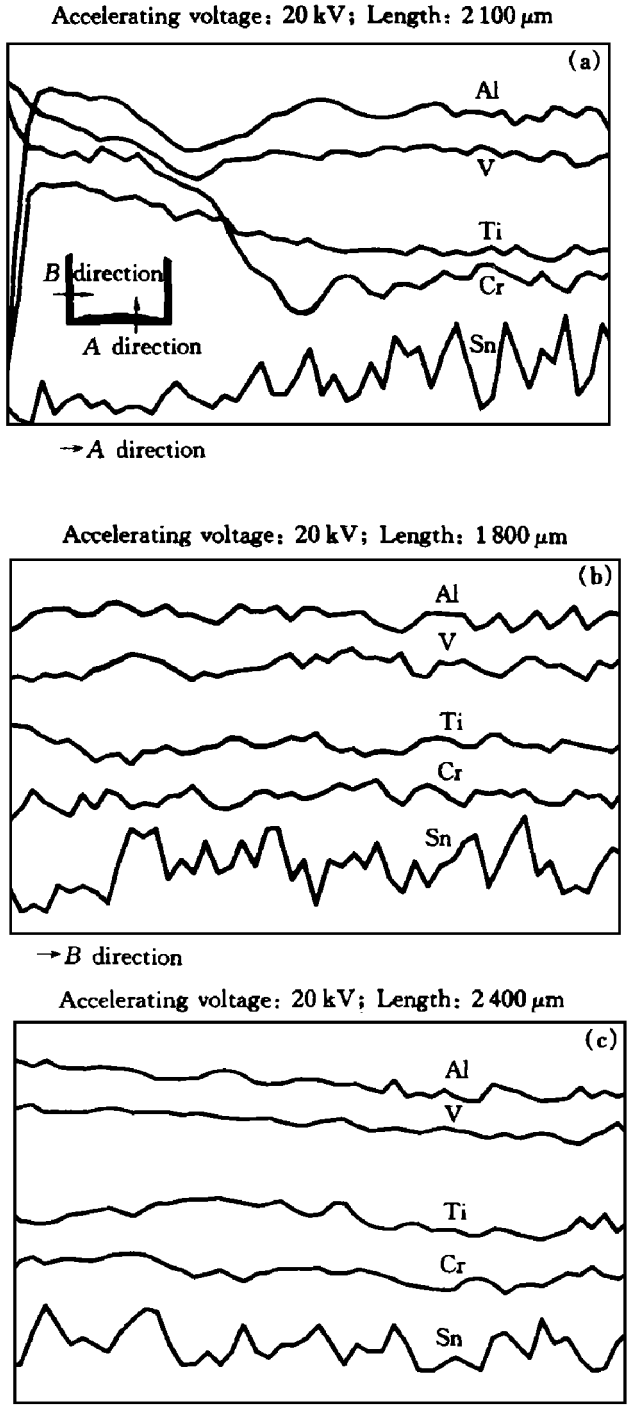

Fig. 6 EPMA to skull side-wall, skull foot-wall as well as ingot obtained from melting practices
(a) —Skull bottom; (b) —Skull wall; (c) —Ingot

tion gradients of all elements in the skull bottom(Fig. 6(a)), especially for Cr and Sn elements, while there is only little fluctuation in the skull wall, which also testifies the fact, that is the macro-segregation of alloying elements concentrates primarily in the skull bottom.

3.4 Formation process of skull

In the incipient stage of the melting process, due to the skin effect of the induction current, the charge near the side wall of the crucible is melted first and flows toward the bottom of the crucible under the action of the electromagnetic force as well as the gravitational force. When the flowing-downwards melt reaches the bottom of the crucible and touches the bottom of the crucible through the gaps between the

unmelted particles, it solidifies and forms the original skull bottom in which there are some unmelted particles. During the flowing process, due to the high density of Cr as well as its shape of powder, it tends to flow with the liquid fluid towards the bottom of the crucible, as a consequence, the enrichment of Cr element in the skull bottom is formed. In addition, because Sn element is not charged into the crucible until the other raw materials have been melted partly, in other words, at this time, the original skull bottom has formed or formed partly; so the poverty of Sn element in some parts of the skull bottom is inevitable, but with the melting process going on, its poverty degree could be weakened owing to the decreasing thickness of the skull bottom and the diffusion of Sn element. Compared with the macro-segregation of Cr and Sn elements, macro-segregations of Ti, V and Al in the skull bottom is slight because on one hand, Ti and the $V_{0.85}Al_{0.15}$ master-alloy are mixed completely; on the other hand, they melt synchronously.

The original skull bottom is thicker. The melting of these unmelted particles in it and the reduction of its thickness depend on the rising temperature in the inner melt. So if the temperature in the inner melt is not high enough, in other words, the melting power is not high enough, even at the end of the melting process, there would be some remnant unmelted particles in the skull bottom, especially in the middle part of the skull bottom because of the lower induction heat and the higher cooling intensity here. Just due to the special formation process of the skull bottom, there must be a certain degree macro-segregation of the alloying elements.

The formation process of the skull wall is different from that of the skull bottom. When the flowing-downwards melt reaches a certain height, that is, when the melt static pressure is higher than the electromagnetic pushing force, the melt begins to touch the wall of the crucible, consequently, a layer of solid skull wall made up of very fine chilled structure is formed. With the above charge melting into the molten pool, the depth of the molten pool increases, as a result, the height of the skull wall increases. When the above charge is wholly melted, the height of the skull wall increases to its maximum value as shown in Fig. 3(a). Then in the later melting process, the rise of the melting power increases the height of the electromagnetic stirring hump, accordingly reduces the contact area between the melt and the wall of the crucible, as the ultimate result, the height of the skull wall decreases.

It can be predicted from the formation process of the skull wall that in the lower position of the skull wall, the macro-segregation of alloying elements is similar to that in the skull bottom because in these parts the skull is made from these firstly melted elements. But with increasing volume of the melt, the melt has already had the nominal composition of the alloy. Moreover the thickness of the skull wall falls with increasing temperature of the inner melt, so in the end, there exists only a little degree macro-segregation of the alloying elements in the skull wall.

4 CONCLUSIONS

The skull microstructure and the elemental line distribution in the skull have been analyzed with optical microscope and EPMA etc. Through the simulation to the temperature field in the charge, the skull shape and size has been predicated and compared with the experimental results. The results show that the skull height and thickness become small with increasing melting power. At the end of the melting process, the thickness of the skull wall and the skull bottom is 0.9 mm and 1.4 mm, respectively. The skull microstructure consists of two zones, that is, fine equiaxial crystal zone and coarse columnar crystal zone. EPMA to the skull shows that there is only little fluctuation in the skull wall and the macro-segregation of alloying elements concentrates primarily in the skull bottom, especially for Cr and Sn elements.

REFERENCES

[1] Boger R. New titanium application on the Boeing 777 airplane [J]. JOM, 1992, 44(5): 23.

[2] Boger R. Aerospace application of beta titanium alloys [J]. JOM, 1994, 46(7): 20.

[3] Breslauer E and Rosen A. Relationship between microstructure and mechanical properties in metastable β titanium 15-3 alloy [J]. Materials Science and Technology, 1991(7): 441.

[4] Bomberger H B and Froes F H. The melting of titanium [J]. JOM, 1984, 36(12): 39.

[5] Sears J W. Current processes for the cold-wall melting of titanium [J]. JOM, 1990, 42(3): 17.

[6] Rowe R G and Froes F H. Titanium rapid solidfication — alloys and processes [A]. In: Froes F H and Savage S J eds. Processing of structural metals by rapid solidfication [C]. Materials Park, OH: ASM, 1987. 163~174.

[7] GUO Jing-jie and SU Yan-qing. Optimization of processing parameters during ISM process of Ti-15-3 alloy [J]. Trans Nonferrous Met Soc China, 1999, 9(1): 17.

[8] GUO Jing-jie, WANG Tong-ming and Su Yan-qing. Numerical simulation of ISM process of titanium alloys [J]. Foundry, (in Chinese), 1997(9): 1.

[9] SU Yan-qing, GUO Jing-jie *et al*. Water-cooling crucible vacuum induction melting of γ-TiAl based alloys [J]. Trans Nonferrous Met Soc China, 1998, 8(1): 69.

(Edited by PENG Chao-qun)